
Reinforced Graph of Thoughts: RL-Driven Adaptive Prompting for LLMs

Manuel Noah Riesen

*School of Engineering and Computer Science
Bern University of Applied Sciences
Bern, Switzerland*

manuelnoah.riesen@students.bfh.ch

Peter Alfred von Niederhäusern

*School of Engineering and Computer Science
Bern University of Applied Sciences
Bern, Switzerland*

peter.vonniederhaeusern@bfh.ch

Abstract

Graph of Thoughts (GoT), a generalized form of recent prompting paradigms for large language models (LLMs), has been shown to be useful for elaborate problem solving. By executing a graph of operations, thoughts of the LLM are structured as an arbitrary graph, forming the actual graph of thoughts. Originally, the graph of operations is defined manually, which requires in-depth knowledge about the solution of the problem to solve. Such a static graph of operations is rigid and therefore lacks adaptability. We propose Reinforced Graph of Thoughts (RGoT), an automated approach to the GoT prompting paradigm that leverages reinforcement learning (RL) to adaptively generate a graph of operations from a human-defined set. Results indicate that, under certain constraints, it is possible to construct graphs of operations adaptively to the task's complexity in an automated way.

Code repository:

<https://github.com/mriesen/reinforced-graph-of-thoughts>

Data on request.

arXiv:2605.22195v1 [cs.LG] 21 May 2026

1 Introduction

The use of advanced prompting paradigms such as Chain of Thought (CoT) and Tree of Thoughts (ToT) has been shown to be useful when it comes to deliberate problem solving with Large Language Models (LLMs) (Wei et al., 2024) (Yao et al., 2024).

Graph of Thoughts (GoT) represents a generalized form of such prompting paradigms. The thoughts of an LLM are modeled as an arbitrary graph (Besta et al., 2024).

We propose Reinforced Graph of Thoughts (RGoT) - an automated approach of GoT to enhance both accessibility and adaptability of complex prompting paradigms.

Accessibility Leveraging more advanced prompting paradigms such as GoT comes with the drawback of an increased complexity for the user. Not only is it important to formulate the prompts correctly, but the operations must be composed in the right order as well. By reducing the user’s work to only the definition of the operations, the Graph of Thoughts paradigm becomes more accessible and can be adapted more easily.

Adaptability The Graph of Thoughts framework by Besta et al. (2024) involves the construction of a complete and static graph of operations. Such a graph is rigid in its behavior. Therefore, a static graph of operations may only be applicable to input with strictly defined properties. Moreover, a static graph is unable to adapt to a language model’s nondeterministic output, which harms the system’s resilience against the language model’s entropic nature. Removing the rigidity from the graph of operations by letting an agent construct the graph continuously in an automated fashion, one may overcome such restrictions to a certain degree.

Differentiation to other Approaches While there is another work on automating GoT (Ha et al., 2024), we present a more sophisticated approach that does not rely on logical capabilities of the underlying language model to build a graph of operations. We evaluate on similar tasks as Besta et al. (2024) and Ha et al. (2024) to demonstrate coverage, not to directly compare results, as the approaches differ fundamentally in adaptability.

In contrast to approaches that use graphs to structure multi-agent collaboration or external knowledge retrieval - such as Knowledge Graph of Thoughts (KGoT) (Besta et al., 2025) - our method targets the automated construction of the reasoning topology itself.

2 Background

2.1 Prompting Paradigms

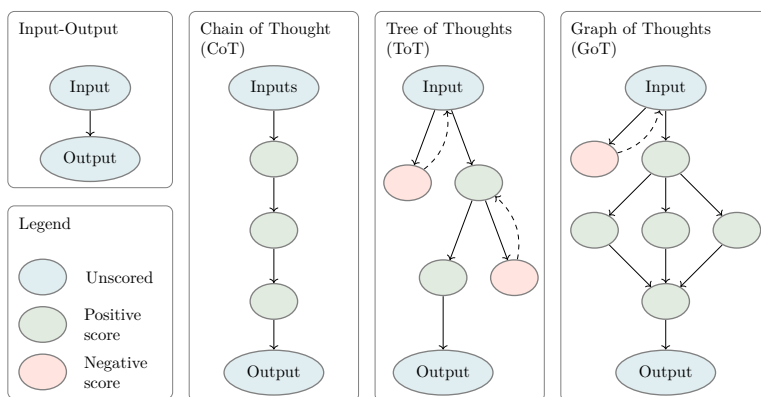


Figure 1: Prompting Paradigms with increasing complexity (from left to right).

Input-Output Prompting The most basic prompting paradigm is the Input-Output (IO) prompting. It describes the interaction between a client (user or system) and a language model, where the client sends a single prompt that is then answered by the language model by a single result (thought).

Chain of Thought Chain of Thought (CoT) (Wei et al., 2024) introduces intermediate reasoning steps in the process of the interaction between the client and the language model. It has been shown that prompting language models to write down the intermediate steps to solve a problem can be beneficial. Besides the benefit of the transparency in the reasoning process, language models may perform better when asked to solve a task step by step.

Tree of Thoughts Tree of Thoughts (ToT) (Yao et al., 2024) introduces a more sophisticated structure for the resulting thoughts of a language model. With ToT, the thoughts are structured as a tree. This allows looking ahead and backtracking within the tree, so that one can navigate to the desired result.

Graph of Thoughts Graph of Thoughts (GoT) (Besta et al., 2024) represents a generalized form of prompting paradigms such as CoT and ToT. Thoughts of the language model are structured as an arbitrary graph. To be precise, GoT is introduced as a framework with its own API definition. A graph of operations acts as the controlling structure. In the original definition, the graph of operations is filled with thoughts until the desired result is achieved. A key novelty with a graph structure in comparison to a tree is the ability to aggregate thoughts. This is highly beneficial for tasks that can be split into simpler subtasks. The subtasks can then be solved locally. Afterwards, the results can be aggregated back into a single combined result. It is also possible to represent preceding prompting structures as graphs of thoughts.

2.2 Reinforcement Learning

Reinforcement Learning (RL) is a subfield of machine learning in which an agent learns by the interaction with an environment (Sutton & Barto, 2018). The problem can be expressed as a Markov Decision Process (MDP). Formally, a MDP is represented by a tuple $(\mathcal{S}, \mathcal{A}, \mathcal{P}, \mathcal{R}, \gamma)$ where \mathcal{S} is the environment’s state space, \mathcal{A} is the agent’s action space, \mathcal{P} is a transition probability function, \mathcal{R} is the reward function and γ is the discount factor. Based on a state $s \in \mathcal{S}$, the agent takes an action $a \in \mathcal{A}$. With a probability of $\mathcal{P}(s' | s, a)$, the agent transitions to the next state $s' \in \mathcal{S}$. After transitioning to state s' , the agent receives the reward given by $\mathcal{R}(s, a, s')$.

Deep Q Learning (DQL) DQL performs Q-Learning (Watkins, 1989) by leveraging a neural network (parameterized with θ) to approximate the (optimal) action-value function $Q^*(s, a)$, so that $Q(s, a, \theta) \approx Q^*(s, a)$ (Mnih et al., 2013). Like the Q-Learning algorithm, it is a model-free and off-policy algorithm.

Advantage Actor Critic (A2C) A2C is an advanced Actor-Critic method, where an advantage function $A(a_t, s_t)$ acts as the critic (Mnih et al., 2016). That is, $A(a_t, s_t) = Q(a_t, s_t) - V(s_t)$ where $Q(a_t, s_t)$ is the action-value function and $V(s_t)$ is the state-value function. $A(a_t, s_t)$ describes the advantage of taking action a_t in state s_t .

Proximal Policy Optimization (PPO) PPO is an Actor-Critic method that is more stable than other algorithms such as A2C (Schulman et al., 2017). PPO uses a clipped "surrogate" objective function L^{CLIP} :

$$L^{\text{CLIP}}(\theta) = \hat{\mathbb{E}}_t \left[\min \left(r_t(\theta) \hat{A}_t, \text{clip} \left(r_t(\theta), 1 - \epsilon, 1 + \epsilon \right) \hat{A}_t \right) \right] \quad (1)$$

with ϵ being a hyperparameter (originally $\epsilon = 0.2$). The first term $r_t(\theta) \hat{A}_t$ corresponds to the L^{CPI} . CPI stands for conservative policy iteration. The clip function clips the probability ratio $r_t(\theta)$ by $1 - \epsilon, 1 + \epsilon$. By doing so, a too large policy update is avoided.

3 Methodology

The work was conducted in multiple phases (Appendix A). For each phase, options were explored (divergence) and then the best option was chosen (convergence).

3.1 The Pure GoT Framework

Instead of relying on the Graph of Thoughts framework of Besta et al. (2024), an adapted one was built on its core concepts (Appendix B). Despite the original framework having an extensible API, its inherent structure does not suit the needs of this automation approach. Our adapted GoT framework aims for simplicity and expressiveness, while enabling processing-independent task definitions and iterative processing.

Task A task is defined as a comprehensive piece of work. A task can be described by a set of possible operations \mathcal{O} .

Operation An operation $o : S^n \rightarrow S^m$ can be seen as a function that transforms incoming states to outgoing states (with n input thoughts and m output thoughts, respectively). An operation can be classified in two variants. 1) A prompt operation is executed by prompting a language model. 2) An execution operation is a programmatically defined function that is evaluated computationally.

Score Operation A score operation $o_s : \mathbb{R} \times S \times S \rightarrow \mathbb{R}$ is applied to get the score of a thought produced by an operation. As input, the score operation receives the cumulative score and both the previous and the current state. The score is represented as a real number. Identical to the common operation, the score operation can either be a prompt operation or a computed execution operation.

Complexity We define complexity as a measurement of difficulty of a task’s instance ¹. It is represented by a numerical value that is specific to a task. The complexity is directly dependent on the input (e.g. number of elements in a list to sum).

Graph of Operations While the reasoning process is modeled in its completeness by Besta et al. (2024), we specify a graph of operations separate from its resulting graph of thoughts and model it with additional constraints (Figure 2a).

A graph of operations is a directed, acyclic graph (DAG) G described by the tuple (V, E) with V being the set of nodes and E being the sets of edges. G is structured into layers L_0, L_1, \dots, L_n , where $n \in \mathbb{N}_0$ and each layer L_i contains a subset of the nodes, such that $V = \bigcup_{i=0}^n L_i$ and $L_i \cap L_j = \emptyset$ for all $i \neq j$. The index of the layer corresponds to the distance of the nodes to the source node. An edge can solely be formed between nodes of directly succeeding layers. That is, for each edge $(u, v) \in E$, if $u \in L_i$ and $v \in L_j$, then $|i - j| = 1$.

G has exactly one source and exactly one sink, so that $|L_0| = 1 \wedge |L_n| = 1$. Having these constraints, G can receive an initial input state and yields a single resulting thought.

By restricting the graph of operations in such a way, the graphs can be treated uniformly.

Graph of Thoughts In this work, the graph of thoughts is separate from the graph of operations, but structured similarly (Figure 2b). However, each thought contains a reference to its creating operation, the thought’s origin (Figure 2c). An exception is the initial state that is wrapped in a thought without origin.

¹In contrary to other definitions such as computational complexity.

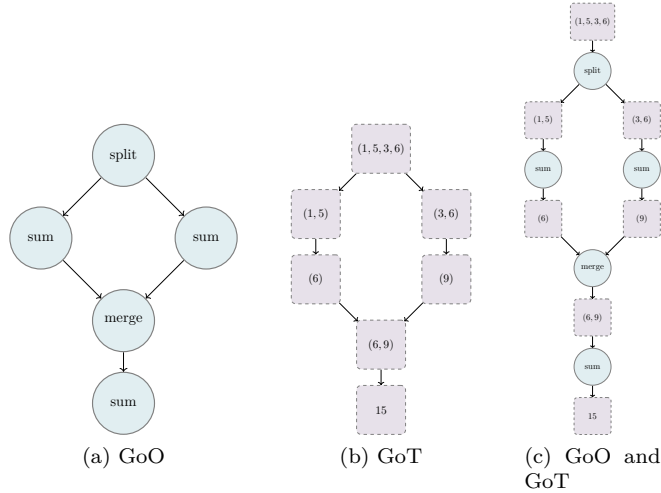


Figure 2: Example GoO, GoT, and their relationship for the task `sum list`.

3.1.1 Application to RGoT

The Pure GoT Framework stands independently and is applied as an external component to RGoT. A custom graph controller allows the step-wise execution of a given graph.

Constraints on Graph Construction Due to the graph of operation’s properties, the graph cannot be constructed completely arbitrarily.

Therefore, certain heuristics are employed to obtain a graph with the desired properties. Both the depth d and the breadth b of the graph must not exceed the maximum depth d_{max} and the maximum breadth b_{max} , respectively. Since a graph of operations must converge towards a single sink, divergence of the graph is not allowed after reaching the divergence cutoff depth d_{div} , which is determined by a divergence cutoff factor μ_{div} :

$$d_{div} = \lceil d \cdot \mu_{div} \rceil \quad (2)$$

Applying these constraints, the construction of a graph of operations is guided towards its proper shape.

3.2 Example Task: `sum list`

In an initial phase, the experiments were conducted on a singular example task named `sum list`, with the goal of calculating the sum of a list of single-digit integers. There are three operations that can be applied in context of the `sum list` task.

- **sum**: calculate the sum of a given list
- **split**: split a given list into equally sized sublists
- **merge**: merge two given lists into a single flat list

The operation `sum` represents the primary operation for solving the task and features an attached computed score operation to evaluate its produced thoughts.

The task `sum list` is chosen as an example task because of its ability to capture the general problem the GoT framework is trying to solve, not because the task represents a real world use case.

Mathematical problem solving is challenging for (conventional) LLMs (Ahn et al., 2024). The task’s complexity can be expressed by the length of the list to sum. The language model’s result is only reliable to a

certain number of elements in the list. Thus, the task can only be solved by the input-output strategy up to a certain list length. Not only must the list’s length be reduced by splitting the list into sublists, but the results must be combined to get the total sum of the list’s elements. The GoT paradigm enables both divergence and convergence of resulting thoughts.

3.3 Additional Tasks

In addition to solving our original example task, we evaluate RGoT on tasks similar to those presented by Besta et al. (2024) (Appendix F).

sort list Sorting a list of single-digit integers. While this is similar in structure as the task **sum list**, this task has different properties in terms of complexity reduction.

intersect set Creating the intersection of two sets. A divide and conquer scheme for set intersection requires a mathematically specific decomposition, which we implemented here statically.

count keywords Counting the number of occurring keywords in a text. Here, the dataset of Besta et al. (2024) is used with custom sampler logic.

merge documents Merging a list of documents into one concise document, while trying to maximize content retention and minimizing redundancy. The dataset of Besta et al. (2024) is used. A noteworthy difference is that we use ROUGE-L for retention scoring and ROUGE-1 for redundancy scoring instead of relying on the language model’s judgment (Lin, 2004).

3.4 LLM Evaluation and Simulation

To overcome the unwanted elasticity of the training cost due to the sample inefficiency of RL, the thoughts of the targeted language model are simulated in the RL environment. The capability of an LLM to solve a task of a given complexity is modeled as a Bernoulli experiment, where each solution attempt succeeds independently with probability $P(c) : \mathbb{N} \rightarrow \mathbb{R}$, with c being the complexity of the task. P is approximated empirically by repeatedly prompting a language model to solve a corresponding task, yielding the estimate $\hat{P}(c) = \frac{n_v}{n}$ with n_v and n being the number of valid results and the total number of results, respectively. We use $n = 100$ per complexity level to fit these estimates. \hat{P} then is used to simulate the behavior of the evaluated LLM during training and evaluation.

Selected Language Models Three language models of OpenAI are used in this work, of which one is chosen (OpenAPI Models) ²:

- `gpt-3.5-turbo-0125`
- `gpt-3.5-turbo-1106`
- `gpt-4-turbo-2024-04-09`

The introduced framework is not limited to OpenAI language models. Any language model can be used by extending the language model API with a respective interface.

Since our framework and automation approach is fully agnostic to the used language model, using more recent models as simulation targets would not give more insights. With the improvement of language models, operations may succeed with higher complexities, which ultimately is just a scaling factor, as post-hoc LLM evaluations show (Appendix H).

²The initial experiments were conducted mid 2024 and the then available models were used. By using those models our experiments are closer to the ones of the original GoT paper of Besta et al. (2024).

3.5 RGoT Reinforcement Learning Configuration

The agent acts on a custom RL environment for GoT construction. The environment is built on an abstraction layer that introduces more specific spaces such as a boolean space and both categorical and ordinal discrete spaces (Appendix D). Experiments with various combinations of network configurations and algorithms, namely DQN, A2C, and PPO, are conducted. The reward function is defined in a reward shaping process that involves empirical evaluation of different reward functions (Wiewiora, 2010).

3.5.1 Action Space

The action space \mathcal{A} is of discrete nature. The agent acts on a layer basis on the graph of operations. Given the set of operations \mathcal{O} , \mathcal{A} is defined as

$$\mathcal{A} = \{stop, backtrack\} \cup \{append(o) \mid o \in \mathcal{O}\} \tag{3}$$

The action *stop* signals the end of the graph of operations and triggers the ground truth evaluation of the result. The sink layer of the graph can be removed by playing the *backtrack* action. A layer with nodes of a certain operation can be appended to the graph by playing the action *append(o)*, where *o* is the operation to append.

3.5.2 Observation Space

The observation space is a composition of multiple discrete spaces, both categorical and ordinal.

$$\mathcal{S} = \mathcal{S}_d \times \mathcal{S}_b \times \mathcal{S}_c \times \mathcal{S}_{lc} \times \mathcal{S}_G \times \mathcal{S}_{pa} \times \mathcal{S}_{ps} \tag{4}$$

Each component provides valuable information about the current state (Table 1).

Component	Notation	Type	Values
Depth	\mathcal{S}_d	Ordinal discrete	$[0, d_{max}]$
Breadth	\mathcal{S}_b	Ordinal discrete	$[0, b_{max}]$
Complexity	\mathcal{S}_c	Ordinal discrete	$[1, c_{max}]$
Local complexity	\mathcal{S}_{lc}	Ordinal discrete	$[1, c_{max}]$
Graph operations	\mathcal{S}_G	Multi discrete	\vec{v}_G
Previous actions	\mathcal{S}_{pa}	Multi discrete	\vec{v}_{pa}
Previous score	\mathcal{S}_{ps}	Optional Boolean	$\{0, 1, \emptyset\}$

Table 1: Observation space components.

Graph Representation The graph of operations is represented in a reduced form based on the graph’s layer. Each layer is represented by the operation of the layer’s nodes. In this scenario, the benefit of reducing the graph’s representation from two dimensions to a single one outweighs the drawback of the lost flexibility. With a lower complexity of the inputs, the agent can learn the impact of the graph structure faster.

4 Results

4.1 LLM Capability Evaluation

Initially, three LLMs were evaluated on the operation `sum` of the task `sum list` (Appendix G.1). Because of its good price-performance ratio, the model `gpt-3.5-turbo-0125` was chosen to be the target model and its \hat{P} was used for the simulation.

The pattern of decreasing probability of success with an increase of complexity is consistent across all critical operations of the example tasks (Figure 3, Appendix G). This property validates and reinforces the use of a prompting paradigm that is capable of divergence and convergence.

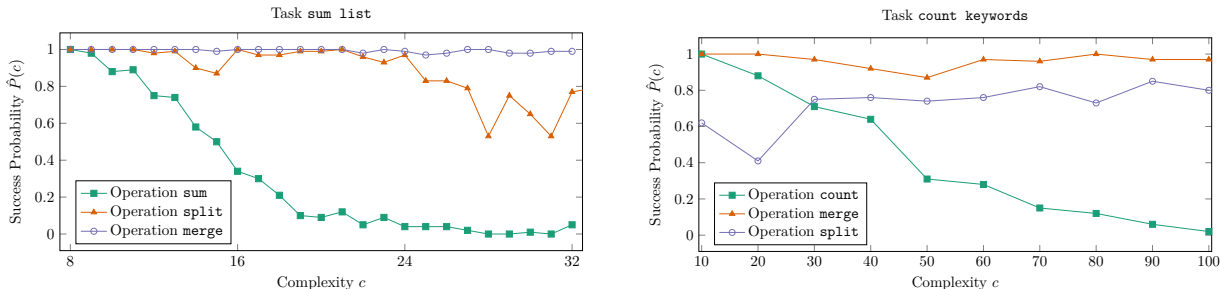


Figure 3: Operation success probability $\hat{P}(c)$ as a function of complexity c for the operations of the tasks `sum list` and `count keywords`, evaluated with `gpt-3.5-turbo-0125`.

4.2 Reinforced Graph of Thoughts Agents

We employ simple PPO agents with 2 layers of 64 units (for both actor and critic network) (Table 2, Appendix I). The agents achieve solid results across all tasks (Figure 4). After 2^{18} training timesteps, the agents are able to solve 0.9399 ± 0.0533 of the training complexities on average across all tasks. Moreover, the agents can solve out-of-distribution complexities, resulting in a total average solved rate³ of 0.7512 ± 0.1089 . In comparison to the input-output (IO) prompting strategy, the agent can solve tasks of higher complexities more reliably.

Hyperparameter	Value
Clip range	linear schedule 0.15 \rightarrow 0.30
Learning rate	linear decay $5 \times 10^{-4} \rightarrow 1 \times 10^{-6}$, 10% warmup
Update epochs K	8
Entropy coefficient	0.03
Policy / value network	[64, 64] / [64, 64]
Total timesteps	2^{18}
Parallel environments	8

(a) PPO hyperparameters.

Parameter	Value
Max steps	20
Max depth d_{max}	8
Max breadth b_{max}	8
Divergence cutoff factor d_{div}	0.5
Max operations	32

(b) Environment parameters.

Table 2: Final PPO and environment configuration.

³Mean solved rate per task computed over all evaluated complexity levels, then averaged across the five tasks

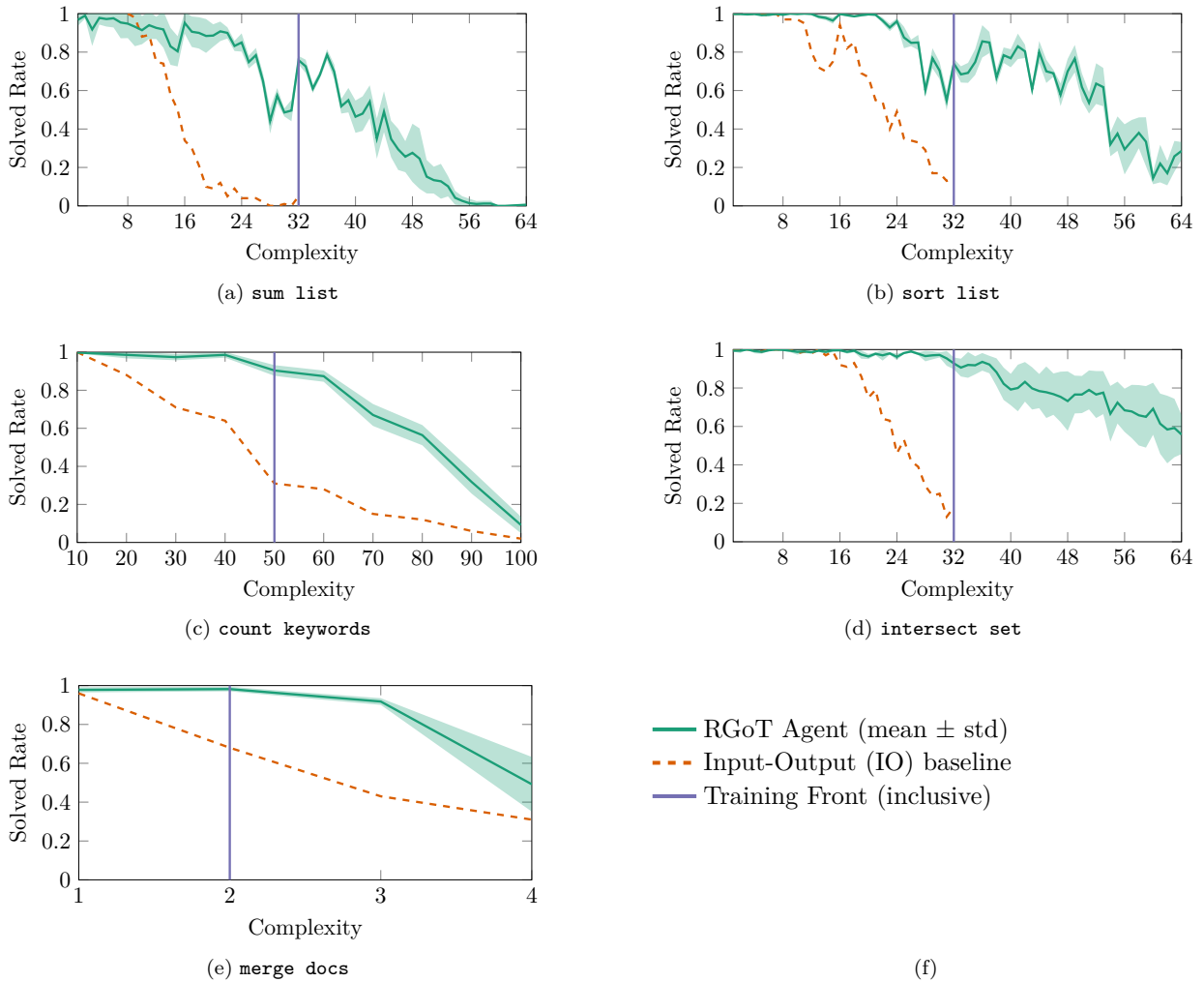


Figure 4: Solved rate per complexity for all five tasks. RGoT agents (teal) are compared against the IO baselines (orange). The vertical line marks the training front, results to its right are out-of-distribution.

5 Discussion

5.1 Agent Performance

There is a generalization of the agent that can be observed. The primary indicator is the number of operations that increases with a higher complexity (Appendix H.1), even after the training front (Figure 4). Despite the absence of the complexities in the training period, the agent decides to increase the branching to solve the task. This leads to the agent’s approach showing a significantly higher solved rate in comparison to the baseline.

Task Complexities One of the key mechanisms for the agent to learn is when to branch instead of applying the primary operation directly. Since the range of complexity levels seen during training is limited, the agent has few opportunities to observe the transition points where decomposition becomes necessary. This may negatively impact generalization, as the agent has limited experience with the branching conditions that dominate at higher complexities.

Variance of Agent Performance Some agents show a higher variance in their performance across different seeds (Figure 4). A possible explanation is a high learning rate sensitivity: as different tasks have different reward landscapes, the applied learning rate schedule may not be optimal for all of them. Another difficulty may be the episode-level noise of the language model simulation. Since the simulation is stochastic, the agent may receive mixed signals for the same graph structure. Furthermore, the sparse reward signal beyond the training front amplifies seed sensitivity: successful episodes become rare at high complexity, so early differences in sampled trajectories can cause the policy to commit to divergent strategies across seeds. This effect lies in the nature of PPO being on-policy: unlike off-policy methods, PPO cannot revisit past successful trajectories and therefore early unlucky seeds cannot recover the missed signal. Consequently, variance is most pronounced in the out-of-distribution region, where the reward signal is weakest and recovery from early suboptimal commitments is least likely.

5.2 Accessibility and Adaptability

By automatically generating a graph of operations, the GoT prompting paradigm is more accessible and requires fewer manual steps and knowledge. More importantly, the agent adapts the operations with respect to the task’s complexity, making the paradigm usable to a broader range of tasks.

5.3 Usability

A key property of RGoT is it being completely language model agnostic. With respect to a task, a language model’s behavior can be simulated by probability distributions of the success of the task’s operations. An agent can then be trained on the desired model’s simulation, offering a cost-effective way of training. When using larger and more capable models only shifts the success range of a task’s operation to higher complexities (Appendix H), one could use smaller models to achieve the same task by using our RL approach.

5.4 Potential Applications

The proposed method is potentially applicable to various tasks that can be solved by a language model, such as merging documents, counting keywords in a text or summarizing large documents.

In the future, it could be possible to create an automated pipeline to train a reinforcement learning agent that can solve a defined task. Additionally, a library of trained agents could be provided for a set of common tasks of a certain domain, so that users can employ the GoT paradigm without additional effort. Moreover, the RGoT approach could be used in combination with Retrieval Augmented Generation (RAG) (Lewis et al., 2020) to both preprocess and postprocess information.

A related direction is Knowledge Graph of Thoughts (KGoT) Besta et al. (2025), which dynamically constructs a knowledge graph to represent the evolving state of an AI assistant task. Since KGoT structures externally retrieved knowledge while RGoT structures the reasoning topology itself, the two paradigms are complementary and could be combined - for example, an RGoT agent could adaptively govern the operation-level structure within a KGoT pipeline.

5.5 Conclusion

To the best of our knowledge, this is the first work to present an automated approach for constructing a graph of thoughts by automatically generating and traversing a graph of operations without relying on a language model’s ability to plan or to know the properties of a presented task. The empirical results indicate that, under certain constraints, it is possible to employ an automated approach to the Graph of Thoughts prompting paradigm by using a reinforcement learning agent.

References

- Janice Ahn, Rishu Verma, Renze Lou, Di Liu, Rui Zhang, and Wenpeng Yin. Large language models for mathematical reasoning: Progresses and challenges. In Neele Falk, Sara Papi, and Mike Zhang (eds.), *Proceedings of the 18th Conference of the European Chapter of the Association for Computational Linguistics: Student Research Workshop*, pp. 225–237, St. Julian’s, Malta, March 2024. Association for Computational Linguistics. URL <https://aclanthology.org/2024.eacl-srw.17>. [cited on page 5]
- Maciej Besta, Nils Blach, Ales Kubicek, Robert Gerstenberger, Lukas Gianinazzi, Joanna Gajda, Tomasz Lehmann, Michał Podstawski, Hubert Niewiadomski, Piotr Nyczyk, and Torsten Hoefer. Graph of thoughts: Solving elaborate problems with large language models. *Proceedings of the AAAI Conference on Artificial Intelligence*, 38(16):17682–17690, 2024. doi: 10.1609/aaai.v38i16.29720. URL <https://ojs.aaai.org/index.php/AAAI/article/view/29720>. Publisher: AAAI Press. [cited on pages 2, 3, 4, 6, and 13]
- Maciej Besta, Lorenzo Paleari, Jia Jiang, Robert Gerstenberger, You Wu, Patrick Iff, Ales Kubicek, Piotr Nyczyk, Diana Khimey, Jón Hannesson, Grzegorz Kwasniewski, Marcin Copik, Hubert Niewiadomski, and Torsten Hoefer. Affordable ai assistants with knowledge graph of thoughts, 2025. [cited on pages 2 and 10]
- Gymnasium. Gymnasium documentation. <https://gymnasium.farama.org/>, 2026. Accessed: Mar. 12, 2026. [cited on page 15]
- Thien-Loc Ha, Trong-Bao Ho, Long Nguyen, and Dien Dinh. Auto graph of thoughts: A hands-free and cost effective method for using graph of thoughts. In *Proceedings of the 2024 10th International Conference on Computer Technology Applications, ICCTA ’24*, pp. 116–121, New York, NY, USA, 2024. Association for Computing Machinery. ISBN 9798400716386. doi: 10.1145/3674558.3674574. URL <https://doi.org/10.1145/3674558.3674574>. [cited on page 2]
- John T. Hancock and Taghi M. Khoshgoftaar. Survey on categorical data for neural networks. *Journal of Big Data*, 7(1):28, 2020. ISSN 2196-1115. doi: 10.1186/s40537-020-00305-w. URL <https://doi.org/10.1186/s40537-020-00305-w>. [cited on page 16]
- Patrick Lewis, Ethan Perez, Aleksandra Piktus, Fabio Petroni, Vladimir Karpukhin, Naman Goyal, Heinrich Küttler, Mike Lewis, Wen-tau Yih, Tim Rocktäschel, Sebastian Riedel, and Douwe Kiela. Retrieval-augmented generation for knowledge-intensive nlp tasks. In *Proceedings of the 34th International Conference on Neural Information Processing Systems, NIPS ’20*, Red Hook, NY, USA, 2020. Curran Associates Inc. ISBN 9781713829546. [cited on page 10]
- Chin-Yew Lin. ROUGE: A package for automatic evaluation of summaries. In *Text Summarization Branches Out*, pp. 74–81, Barcelona, Spain, July 2004. Association for Computational Linguistics. URL <https://aclanthology.org/W04-1013/>. [cited on pages 6 and 22]
- Makoto Matsumoto and Takuji Nishimura. Mersenne twister: A 623-dimensionally equidistributed uniform pseudo-random number generator. *ACM Transactions on Modeling and Computer Simulation*, 8(1):3–30, January 1998. doi: 10.1145/272991.272995. [cited on page 15]
- Volodymyr Mnih, Koray Kavukcuoglu, David Silver, Alex Graves, Ioannis Antonoglou, Daan Wierstra, and Martin A. Riedmiller. Playing atari with deep reinforcement learning. *CoRR*, abs/1312.5602, 2013. URL <http://arxiv.org/abs/1312.5602>. [cited on page 3]
- Volodymyr Mnih, Adria Puigdomenech Badia, Mehdi Mirza, Alex Graves, Timothy Lillicrap, Tim Harley, David Silver, and Koray Kavukcuoglu. Asynchronous methods for deep reinforcement learning. In *International conference on machine learning*, pp. 1928–1937. PMLR, 2016. [cited on page 3]
- Melissa E. O’Neill. PCG: A family of simple fast space-efficient statistically good algorithms for random number generation. Technical Report HMC-CS-2014-0905, Harvey Mudd College, Claremont, CA, September 2014. [cited on page 15]

-
- OpenAPI Models. Models - OpenAI API. <https://platform.openai.com/docs/models/overview>, 2024. [cited on page 6]
- Python. Welcome to python.org. <https://www.python.org/>, 2026. Accessed: Mar. 12, 2026. [cited on page 15]
- Antonin Raffin, Ashley Hill, Adam Gleave, Anssi Kanervisto, Maximilian Ernestus, and Noah Dormann. Stable-baselines3: Reliable reinforcement learning implementations. *Journal of Machine Learning Research*, 22(268):1–8, 2021. URL <http://jmlr.org/papers/v22/20-1364.html>. [cited on page 15]
- John K. Salmon, Mark A. Moraes, Ron O. Dror, and David E. Shaw. Parallel random numbers: as easy as 1, 2, 3. In *Proceedings of 2011 International Conference for High Performance Computing, Networking, Storage and Analysis*, pp. 1–12. ACM, 2011. ISBN 978-1-4503-0771-0. doi: 10.1145/2063384.2063405. URL <https://dl.acm.org/doi/10.1145/2063384.2063405>. [cited on page 15]
- John Schulman, Filip Wolski, Prafulla Dhariwal, Alec Radford, and Oleg Klimov. Proximal policy optimization algorithms. *arXiv preprint arXiv:1707.06347*, 2017. [cited on page 3]
- Stable Baselines3. Developer guide — Stable Baselines3 2.3.2 documentation. <https://stable-baselines3.readthedocs.io/en/master/guide/developer.html>, 2026. Accessed: Mar. 15, 2026. [cited on page 16]
- Richard S Sutton and Andrew G Barto. *Reinforcement Learning, Second Edition*. The MIT Press, 2018. ISBN 978-0-262-36401-0. [cited on page 3]
- Christopher Watkins. *Learning from Delayed Rewards*. PhD thesis, King’s College, Cambridge, 1989. [cited on page 3]
- Jason Wei, Xuezhi Wang, Dale Schuurmans, Maarten Bosma, Brian Ichter, Fei Xia, Ed H. Chi, Quoc V. Le, and Denny Zhou. Chain-of-thought prompting elicits reasoning in large language models. In *Proceedings of the 36th International Conference on Neural Information Processing Systems, NIPS ’22*, Red Hook, NY, USA, 2024. Curran Associates Inc. ISBN 9781713871088. [cited on pages 2 and 3]
- Eric Wiewiora. Reward shaping. In Claude Sammut and Geoffrey I. Webb (eds.), *Encyclopedia of Machine Learning*, pp. 863–865. Springer US, 2010. ISBN 978-0-387-30164-8. doi: 10.1007/978-0-387-30164-8_731. URL https://doi.org/10.1007/978-0-387-30164-8_731. [cited on page 7]
- Shunyu Yao, Dian Yu, Jeffrey Zhao, Izhak Shafran, Tom Griffiths, Yuan Cao, and Karthik Narasimhan. Tree of thoughts: Deliberate problem solving with large language models. *Advances in Neural Information Processing Systems*, 36, 2024. [cited on pages 2 and 3]

A Project Structure

The project consists of two phases (Figure 5).

Initial phase In a first phase, the operation `sum` of the task `sum list` was evaluated on different language models, of which then `gpt-3.5-turbo-0125` was selected. Different RL algorithms were then evaluated with a variety of configurations, of which one PPO was selected for further tuning. This provided a foundation for further experiments.

Expansion phase Since a single example task is not representative, it was decided to extend the set of tasks with tasks similar to the ones shown by Besta et al. (2024). Moreover, all operations were evaluated on `gpt-3.5-turbo-0125`. Then, for each task a PPO agent was trained.

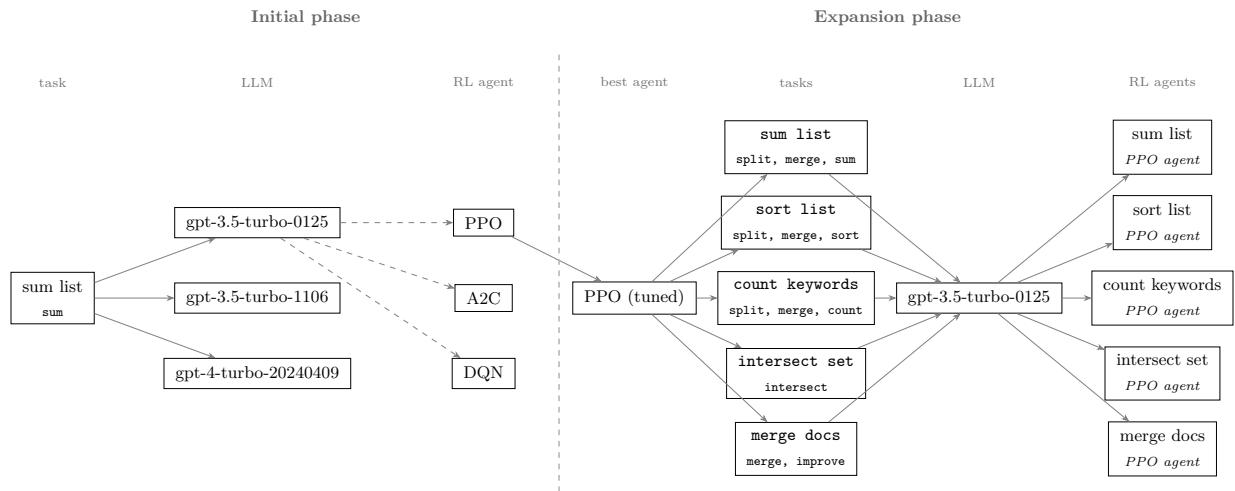


Figure 5: Project Structure

B Pure Graph of Thoughts

Our Pure Graph of Thoughts framework addresses the absence of some functionalities of the original GoT framework and represents the foundation for the RGoT framework.

As a user-facing API, operations can be defined in a declarative way over a typed and validated data structure (DSL) (Figure 6). This allows the definition of operations and tasks decoupled to the underlying processing. There is a strict distinction between a prompt operation executed by a language model and a code execution operation. To simplify parsing logic and to ensure consistent results, the JSON format is used for communication with the language model. The scoring is now part of an operation involving a prompt, rather than being a standalone operation that can be added arbitrarily. While this simplifies the automation process, it restricts the user’s possibility of adding a validation operation. While the framework is crafted with automation in mind, it allows the manual construction of graphs of operations. Operations and thoughts are represented independently of their graph structure.

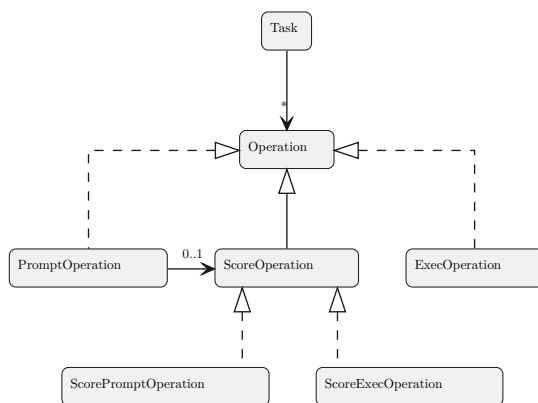


Figure 6: Pure Graph of Thoughts Types

The related code can be found in the following repository: <https://github.com/mriesen/pure-graph-of-thoughts>

C Technical Details

C.1 Randomness

In the context of this work, whenever reference is made to randomly generated numbers or structures, it is always referred to pseudo-random numbers generated by a pseudo-random number generator (PRNG). More specifically, Mersenne Twister (Matsumoto & Nishimura, 1998) (Python default) and PCG (O’Neill, 2014) (NumPy default) are used for CPU-based pseudo-random number generation, whereas the pseudo-randomness on GPU devices is sourced from the Philox algorithm (Salmon et al., 2011) (PyTorch default).

To ensure reproducibility, the PRNGs are used with a fixed seed. For the language model evaluation, the seed 0 is used. The training and evaluation of the RL agents incorporates multiple seeds, of which the seed set $\{0, 8, 16, 24, 32\}$ is specified. The RL training uses 8 vectorized environments, where each of the environments uses its own seed derived by addition of the specified seed and the rank $[0..8[$. This leads to the use of all seeds in $[0..32[$ (with some exceptions ⁴).

C.2 Technological Overview

The source code of this work is produced in Python, using the defined APIs and libraries (Table 3) (Python).

For the RL environment definition, the Gymnasium API is used, which is a widely used standard (Gymnasium).

Where possible, the RL algorithm implementations of Stable Baselines3 are used. Stable Baselines3 provides reliable implementations of common RL algorithms in PyTorch (Raffin et al., 2021).

Name	Usage
Python	Programming language
Gymnasium	API standard for RL environment definition
Stable Baselines3	Implementations of RL algorithms

Table 3: Technological Overview

⁴The seeding of the language model simulators is decoupled by adding 10^5 to it.

D RL Observation Space Types

Instead of forming the observation space directly out of the spaces defined by Gymnasium, an abstraction layer is put on top. This allows more specific definitions of spaces (Table 4).

Categorical vs ordinal discrete spaces When it comes to encoding categorical data, one-hot encoding is chosen over a numeric encoding in the form of integers or continuous values. This applies for both the actions and the observations of the reinforcement learning environment. Numeric encoding is more space efficient, but introduces an ordinal relationship between the categories. In the case of independent, unordered categories, such ordinal relationships increase the complexity for the underlying model and may have an impact on the model’s performance. While the one-hot encoding is less space efficient than numeric encoding, it does not introduce an ordinal relationship between the categories. Thus, it represents the categories better than numeric encoding, which may be the reason it is widely used (Hancock & Khoshgoftaar, 2020).

By default, Stable Baselines3 converts the Gymnasium space *Discrete* into one-hot vectors (Stable Baselines3).

However, in some cases it is beneficial to have an ordinal relationship for discrete values. The implementation of the ordinal discrete space is achieved by using a continuous space (called *Box*) and by mapping the discrete values to a continuous value between -1 and 1 .

Boolean and optional Boolean The Boolean space is implemented with a multi-binary space that consists of a single bit. For the optional Boolean space, a categorical discrete space with 3 categories is used.

Space Type	Values
Categorical discrete	$\{\vec{v} \in \{0, 1\}^n \mid \sum_{i=1}^n \vec{v}_i = 1\}$
Ordinal discrete	$\{x \in \mathbb{R} \mid -1 \leq x \leq 1\}$
Multi discrete	$\{M \in \{0, 1\}^{m \times n} \mid \forall j \in \{1, 2, \dots, n\}, \sum_{i=1}^m M_{ij} = 1\}$
Continuous	\mathbb{R}
Boolean	$\{0, 1\}$
Optional Boolean	$\{\vec{v} \in \{0, 1\}^3 \mid \sum_{i=1}^3 \vec{v}_i = 1\}$

Table 4: Observation Space Types

E Reward Function

During the reward shaping, several different reward functions were evaluated. As a result, the version 7 performed best (Algorithm 1). Note that the output is scaled by factor of $\frac{1}{100}$ as a normalization measurement.

Algorithm 1 Reward Function Version 7

```
1: penaltydepth  $\leftarrow -\left(\frac{10}{\text{depth}_{\max}}\right) \times \text{depth}$ 
2: if invalid then
3:   return -10
4: end if
5: if action = backtrack then
6:   if scoredprev  $\neq$  None and not scoredprev then
7:     return 15
8:   else
9:     return -10
10:  end if
11: end if
12: if operation is not scored then
13:   return 10 + penaltydepth
14: end if
15: if score then
16:   if final then
17:     return 100
18:   else
19:     return 10 + penaltydepth
20:   end if
21: end if
22: if final then
23:   return -20 + penaltydepth
24: end if
25: return -10 + penaltydepth
```

F Task Definitions

F.1 Task sum list

The task `sum list` aims to calculate the sum of a list of single-digit integers. The complexity is defined as the number of elements in the list.

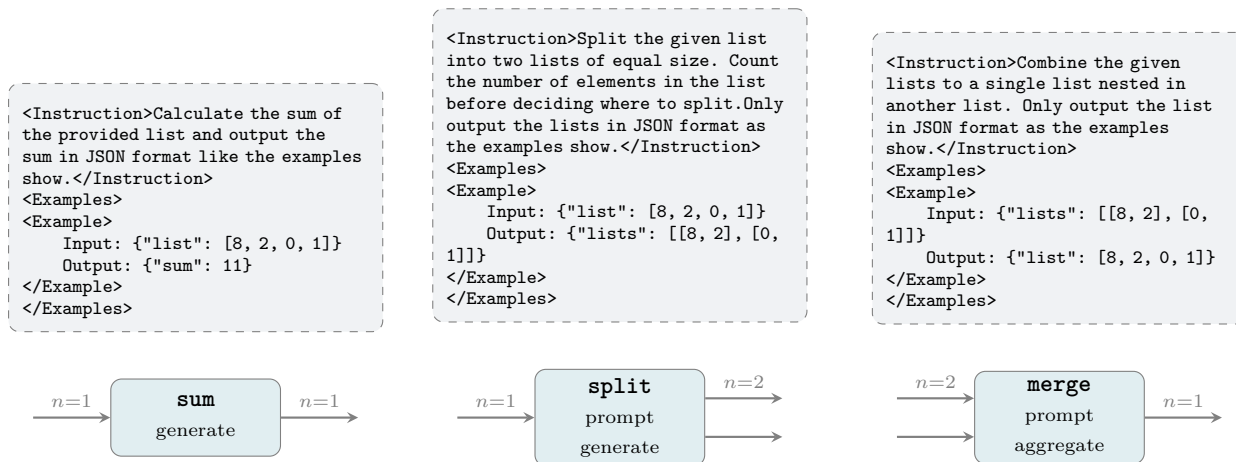


Figure 7: Operations of task `sum list` with input/output arities and prompt descriptions.

Operation `sum` For a given list of single-digit integers, the sum is to be calculated (Listing 8). The scoring is based on whether the sum is correct.

```

op_sum = PromptOperation(
  name='sum',
  n_outputs=1,
  n_inputs=1,
  type=OperationType.GENERATE,
  output_complexity=absolute_complexity(1),
  prompt=Prompt(
    instruction='Calculate the sum of the provided list and output the sum in JSON format like the examples show.',
    examples=[
      Example(
        input={
          'list': [8, 2, 0, 1]
        },
        output={
          'sum': 11
        }
      )
    ]
  ),
  transform_before=lambda states: {
    'list': []
  } if len(states) == 0 else {
    'list': [states[0]['sum']]
  } if 'sum' in states[0] else states[0],
  score_operation=ScoreExecOperation(
    name='score_sum',
    type=OperationType.SCORE,
    score=score_op_sum,
    n_inputs=1,
    n_outputs=1
  )
)

```

Figure 8: Definition of Operation `sum`

Operation `split` A list is to be split into two equally sized sublists. The scoring is based on whether the output contains two similarly sized lists, with some lenience (sublist ratio ≥ 0.5).

Operation `merge` Two given lists are to be merged into a single list. The result is scored based on whether the sum of the resulting list equals the sum of the input sublists and on the correct size of the merged list.

F.2 Task sort list

The goal of the task `sort list` is to sort a list of single-digit integers. The complexity is defined as the number of elements in the list.

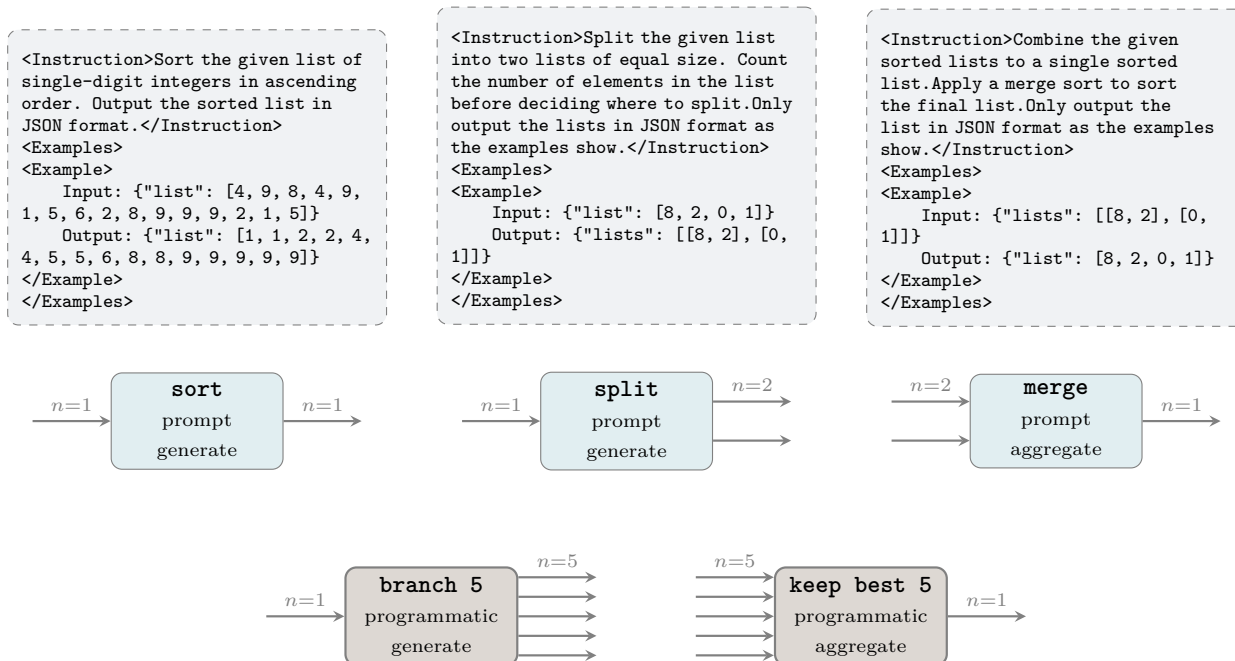


Figure 9: Operations of task `sort list` with input/output arities and prompt descriptions.

Operation sort A given list is to be sorted in ascending order. The number of sort errors is calculated and the (binary) scoring strictly allows no errors.

Operation split Identical to the Operation `split` of Task `sum list`.

Operation merge Identical to the Operation `merge` of Task `sum list`.

Operation branch 5 A programmatic operation that copies the state 5 times.

Operation keep best from 5 A programmatic operation that selects the best of the incoming states.

F.3 Task intersect set

This task aims to build the intersection of two sets. The complexity is defined as the number of elements in the set.

```

<Instruction>Find the intersection
of two given sets of integers.Output
only the numbers that are present
in both input sets in JSON
format.</Instruction>
<Examples>
<Example>
  Input: {"set1": [1, 5, 8, 2],
"set2": [2, 4, 5, 9]}
  Output: {"intersection": [2,
5]}
</Example>
</Examples>

```

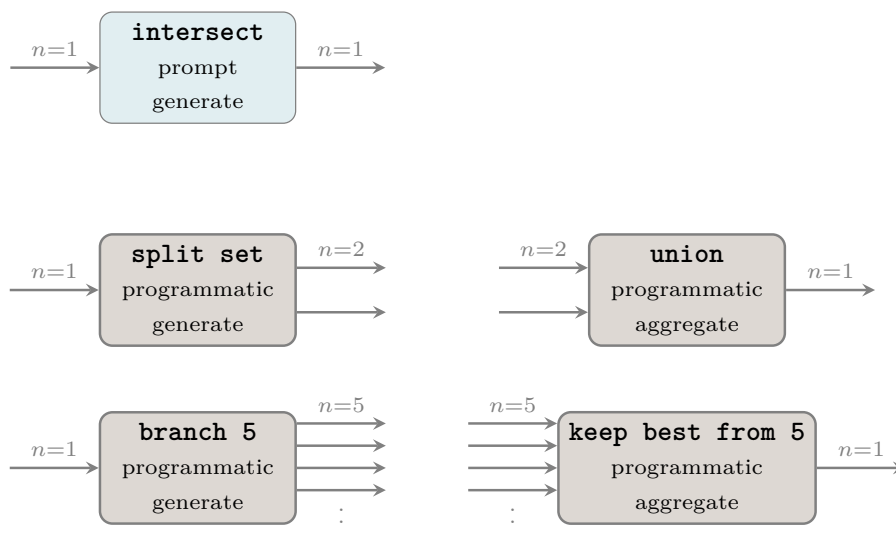


Figure 10: Operations of task `intersect set` with input/output arities and prompt descriptions.

Operation intersect The intersection of a set is to be created. The scoring is based on whether the intersection of the sets is correct.

Operation split set Given two sets as input (a single state), two states are created: The first set is split in half, the subsets are fed as first set into the respective output states, including the second (unmodified) set.

Operation union Given two states, the union of the sets is created.

Operation branch 5 Copies the state 5 times.

Operation keep best from 5 Selects the best state from given 5 states.

F.4 Task count keywords

The goal is to count the keywords in a given text. With the type of keywords defined (here: countries), the language model is advised to count the number of occurrences of the keywords (count per keyword). The complexity is defined as the number of words in the text to count keywords of.

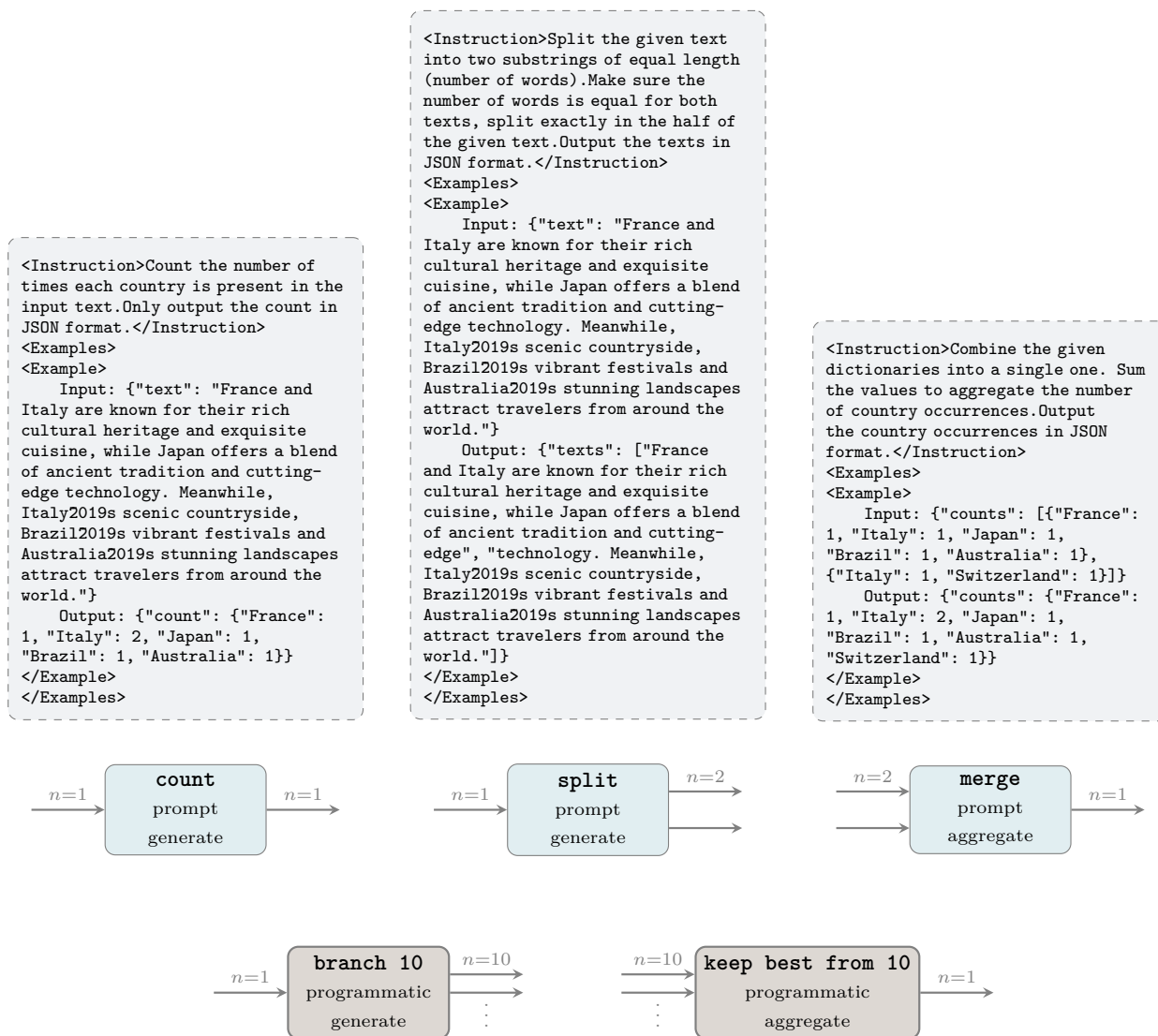


Figure 11: Operations of task count keywords with input/output arities and prompt descriptions.

Operation count Given a text, the number of specific words (here: countries) is to be counted. The scoring is based on whether the words are counted correctly.

Operation split Given a text, it is to be split into two substrings of similar size. Here, the scoring is dependent on whether the text is split correctly and in two similarly sized parts, given some lenience (text ratio ≥ 0.25).

Operation branch 10 Copies the state 10 times.

Operation keep best from 10 Selects the best state from given 10 states.

F.5 Task merge docs

The goal of `merge docs` is to merge a set of documents into a single document. The complexity is defined as the number of documents to be merged.

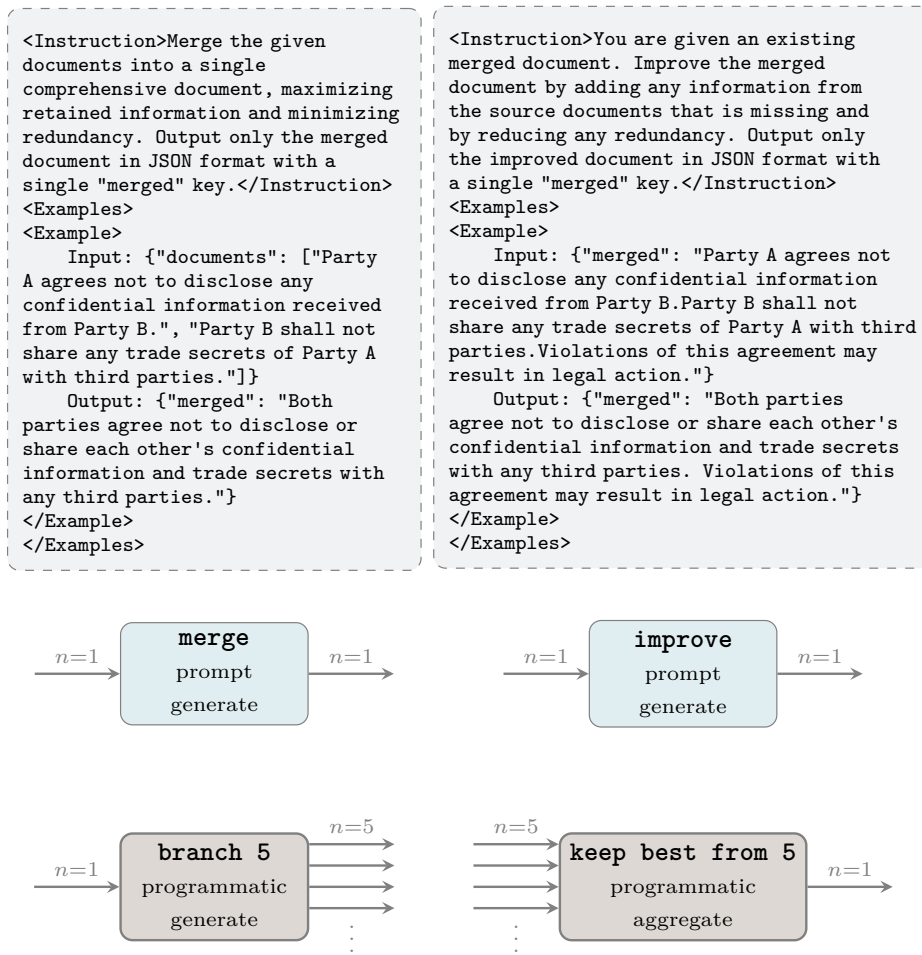


Figure 12: Operations of task `merge docs` with input/output arities and prompt descriptions.

Operation merge Several documents are to be merged into a single one, while minimizing redundancy and maximizing information retention. The scoring is based on the ROUGE-L (retention) and ROUGE-1 (redundancy) score and the resulting F1 score Lin (2004). To decide whether a result is valid, we used the threshold 0.6, which was determined empirically⁵. In practice, this threshold can be modified based on the use case.

Operation improve A merged document is to be improved in terms of information retention and redundancy minimization. The scoring is identical to the `merge` operation. Since we only have one document, the only complexity to be seen is 1.

Operation branch 5 Copies the state 5 times.

Operation keep best from 5 Selects the best state from given 5 states.

⁵Using the F1 threshold of 0.6 for the `merge` operation, language model evaluations showed a linear decrease of valid results with an increase of the number of documents to merge.

G LLM Capability Evaluation

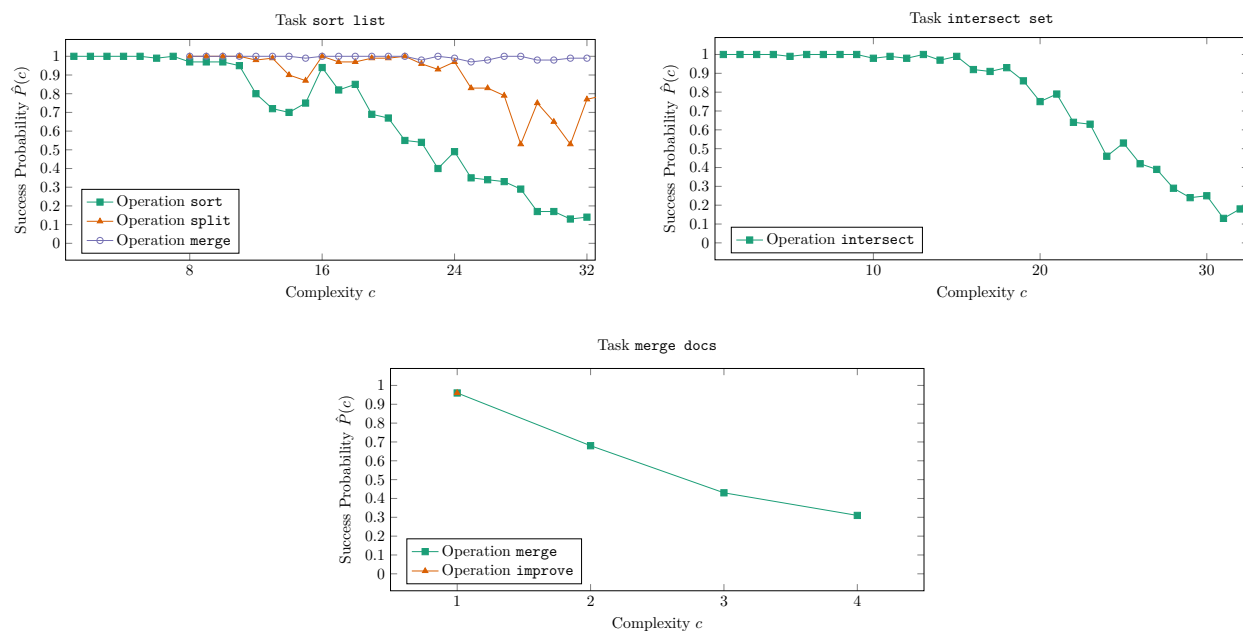


Figure 13: Operation success probability $\hat{P}(c)$ as a function of complexity c for each task, evaluated with gpt-3.5-turbo-0125.

G.1 Initial LLM Evaluation

The operation sum of the task sum list was initially evaluated on different language models. The variants of gpt-3.5-turbo are quite on-par in solving the specified task. The model gpt-4-turbo-2024-04-09 maintains a higher success rate before degrading similarly (Figure 14).

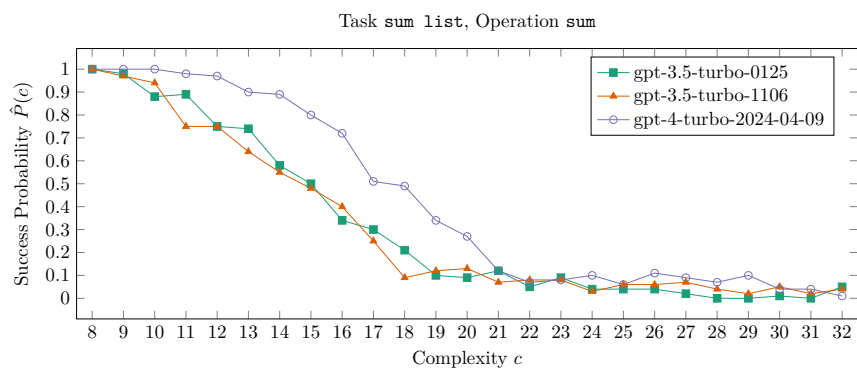


Figure 14: LLM Evaluation Results for Operation sum of Task sum list (with $n = 100$)

H Post-Hoc LLM Evaluation

To verify that recent LLMs also show a degradation with an increase of a task’s complexity, two modern models were evaluated after the training of the RL agents (Figure 15). We extended the evaluation up to list size 48 (50% more than before), as the assumption was that the newer models perform better. The results clearly show that while the models can keep up a higher success rate longer, they still degrade after a certain number of list elements.

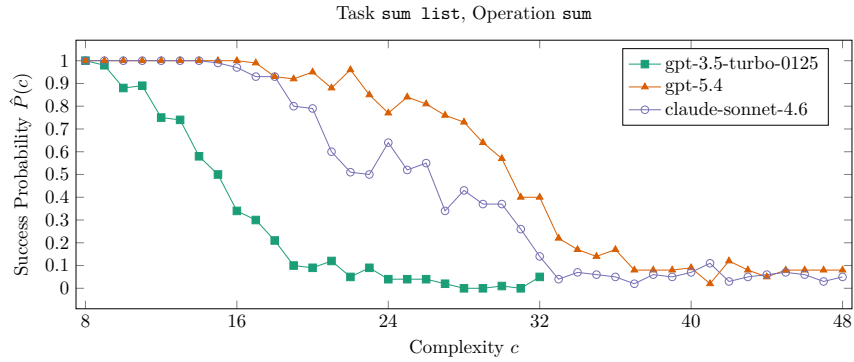


Figure 15: LLM Evaluation Results for Operation sum of Task sum list (with $n = 100$)

H.1 Agent Evaluation Results

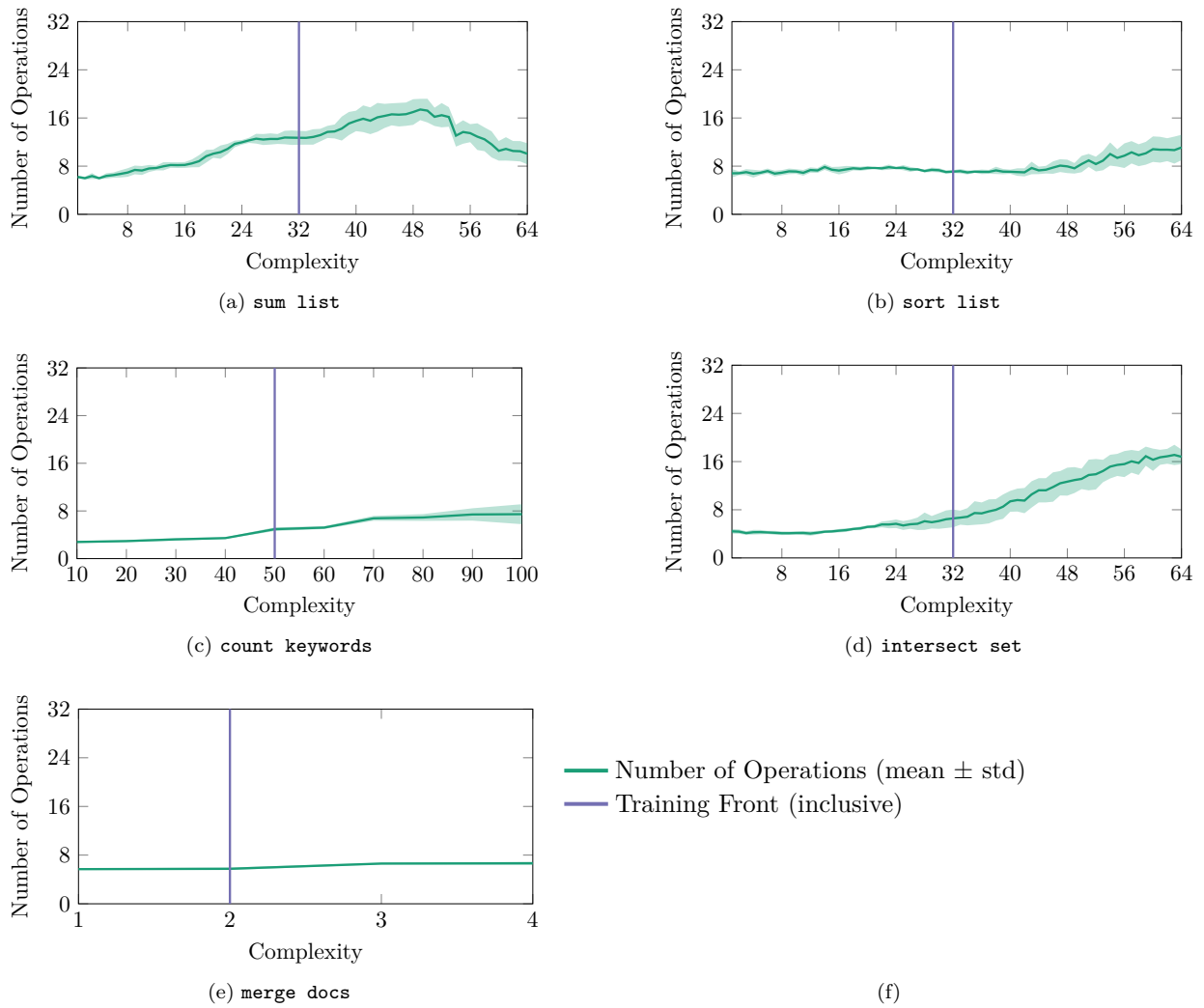


Figure 16: Number of operations per complexity for all five tasks. The vertical line marks the training front, results to its right are out-of-distribution.

I Ablation Summary

In the expansion phase, we conducted a search over PPO hyperparameters. The findings are summarized below.

Clip range We introduced a clip range schedule annealing from 0.15 to 0.3 over the training.

A fixed low clip caused destructive early policy updates; the schedule reduces seed sensitivity significantly. Values above 0.3 showed no benefit.

Update epochs We evaluated $K \in \{5, 8, 10\}$ epochs per rollout batch. $K = 8$ was optimal. $K = 10$ introduced instability on some tasks with negligible gain elsewhere.

Learning rate Among the schedules compared, linear decay performed better than cosine decay. A warmup over the first 10% was added, dampening the impact of noisy early gradient steps.

Final schedule: linear decay from $\alpha_0 = 5 \times 10^{-4}$ to $\alpha_T = 1 \times 10^{-6}$ with warmup 10%.

Total timesteps $2^{18} = 262,144$ timesteps was used throughout. Doubling to 2^{19} caused collapse on several tasks, potentially due to the learning rate schedule decaying too slowly over the longer period.

Network architecture Compared $[64, 64]$ and $[128, 64]$ for both policy and value networks. There was no significant benefit of employing the larger network, therefore $[64, 64]$ represents the final configuration.

Entropy coefficient Set to 0.03 to maintain sufficient exploration throughout training without destabilizing the policy.